Investigation of WO_3/ZnO thin-film heterojunction-based Schottky diodes for H_2 gas sensing

Y. Liu, J. Yu, P.T. Lai

Department of Electrical and Electronic Engineering, The University of Hong Kong, Hong Kong, China

Abstract

A comparative study of Schottky diode hydrogen gas sensors based on Pd/WO_3/Si and Pd/WO_3/ZnO/Si structure is presented in this work. Atomic force microscopy and X-ray photoelectron spectroscopy reveal that the WO_3 sensing layer grown on ZnO has a rougher surface and better stoichiometric composition than the one grown on the Si substrate. Analysis of the *I-V* characteristics and dynamic response of the two sensors when exposed to different hydrogen concentrations and various temperatures indicate that with the addition of the ZnO layer, the diode can exhibit a larger voltage shift of 4.0 V, 10 times higher sensitivity, and shorter response and recovery times (105 s and 25 s, respectively) towards 10,000-ppm H_2/air at 423 K. Study on the energy band diagram of the diode suggests that the barrier height is modulated by the WO_3/ZnO heterojunction, which could be verified by the symmetrical sensing properties of the Pd/WO_3/ZnO/Si gas sensor with respect to applied voltage.

Keywords: Schottky diode, hydrogen sensor, heterojunction, ZnO, WO_3

1. Introduction

With the rapid development of hydrogen economy over the last three decades [1], increasing attention has been drawn to hydrogen safety issues. The properties of low ignition energy (0.017 mJ), wide flammable range (4% ~ 75%) and high diffusion coefficient (0.61 cm^2/s) [2] all suggest the risks of hydrogen leakage. Therefore, an accurate and rapid hydrogen sensor, in early warning systems to prevent explosion, is an essential complimentary device during its production, storage, transportation and usage in domestic as well as industrial applications.

The structure of Schottky diode based gas sensors usually consist of an interfacial metal-oxide layer to increase gas sensitivity and provide thermal dynamic stability over their electrical characteristics [3,4]. Compared with SiC- or GaN-based hydrogen sensors, Si-based devices remain with numerous benefits, owing to their low cost, low power consumption and compatibility with modern integrated electronic systems [5,6]. Much research has shown that various metal oxide materials including MoO_3, SnO_2, HfO_2, ZnO and WO_3 [7-10], with different microstructures, can be considered in the design of hydrogen sensors. Amongst

these oxides, WO_3, is one of the most attractive materials which shows gas sensitivities covering a wide range of concentrations and fast response as well as good selectivity [11]. As for conventional WO_3 thin film prepared on Si substrate, however, defects originating from oxygen vacancies can pin the Fermi level and hinder the sensing performance of such Schottky diode sensors that rely on the barrier height variation [12].

To reduce the presence of defects, an intermediate WO_3/ZnO heterojunction layer was deposited between the Schottky contact metal and the semiconducting substrate. We expect the potential difference across such a heterojunction can attenuate the drift mobility of the electrons flowing in the opposite direction and increase the effective Schottky energy barrier, and thus enhance the gas sensing performance and shorten the response [13,14]. In this work, we study and compare the hydrogen sensing properties of two Schottky diodes with Pd/WO_3/Si and Pd/WO_3/ZnO/Si configurations. Experimental results show that with the implementation of a WO_3/ZnO heterostructure in the diode, it exhibits better performance as a sensor in both forward and reverse biases, faster response and higher sensitivity.

2. Experimental

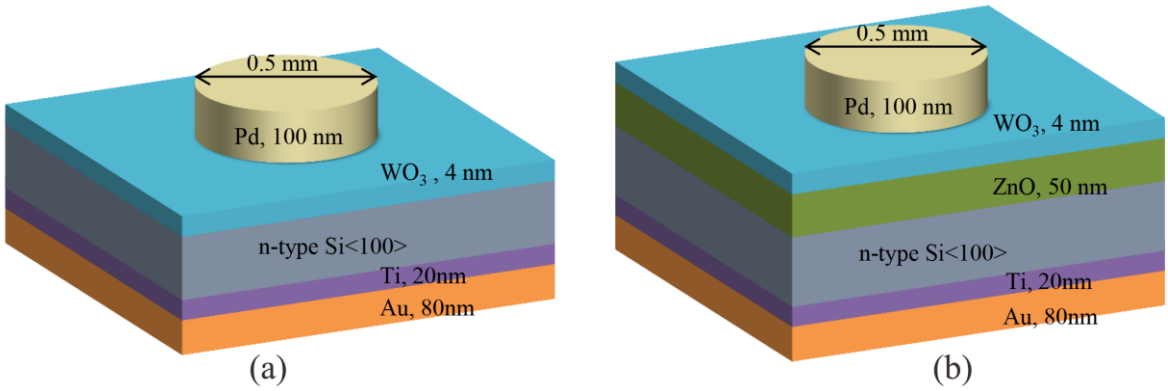

FIG. 1. Schematic cross section of the (a) Pd/WO3/Si and (b) Pd/WO3/ZnO/Si Schottky diodes

The fabrication of the Schottky diodes for this study was conducted using <100> *n*-type Si wafers (Silicon Quest International, USA) with resistivity of 0.5 ~ 1.0 Ω.cm. The wafers were first diced into 7 mm×7 mm squares and cleaned using the RCA method to remove both organic and inorganic artifacts. The native oxide was removed by etching in 5 % hydrofluoric acid in de-ionized water for at least 1 minute. A 20 nm/80 nm thick Ti/Au metal contact was deposited on the backside of the silicon substrate via e-beam evaporation, and heat treatment was performed in a rapid annealing furnace (RTA) at 1123 K for 90 seconds in nitrogen to form the ohmic contact. To remove excess artifacts, the metalized substrates were placed in an ultrasonic cleaning bath with acetone and isopropanol solutions, and subsequently loaded into Denton Vacuum sputterer, where ZnO and WO_3 thin films were obtained by RF sputtering. Subsequently, the samples were treated with a second annealing process at 823 K for one hour in synthetic air to stabilize the oxide layers and decrease their defects. The samples were then cleaned with acetone and isopropanol prior to depositing a 100 nm thick palladium contact using a stainless steel shadow mask with a diameter of 0.5

mm via DC sputtering onto the WO_3 layer. A third annealing process was performed at 573 K for 10 minutes in nitrogen to stabilize the formation of the Schottky contact. Following these processing steps, the samples were pasted with silver epoxy onto standard TO-8 gold headers and the Schottky and ohmic metals were connected to the header pins via Au wire bonding. Figure 1 shows the configuration of the final devices. The thickness of the oxide layers was determined by VASE ellipsometer.

The electrical characteristics of studied devices were measured by a HP 4145B semiconductor analyzer. All hydrogen-sensing tests were performed in a system consisting of a stainless chamber isolated from external atmosphere and moisture, a programmable gas-mixing system and a computer-controlled oven.

3. Material characterization

3.1 Atomic force microscopy analysis

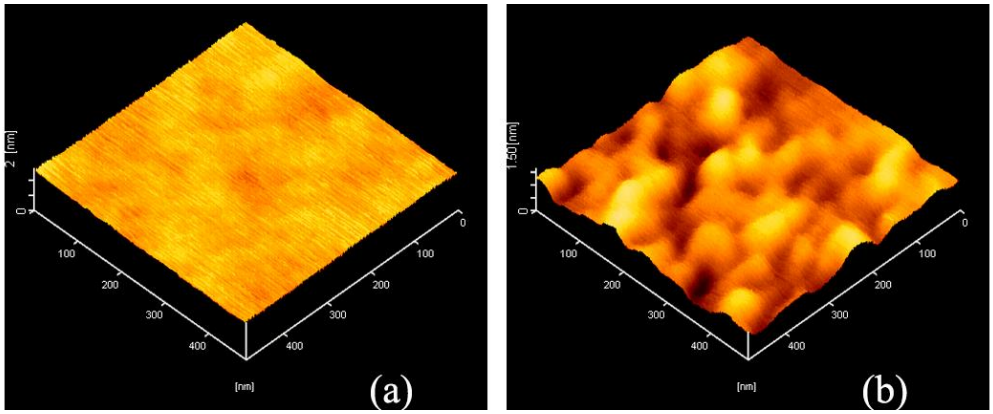

FIG. 2. AFM micrographs of the sputtered WO_3 surface as grown on (a) Si and (b) ZnO

To study the top WO_3 thin film and their interface with the underlying layer (Si or ZnO), the surface morphology of the WO_3 layer was mapped using atomic force microscopy (AFM) as shown in figure 2. The AFM images show that WO_3 grown on ZnO is significantly rougher than the WO_3 grown on Si. The root-mean-square (RMS) roughness of WO_3/Si and WO_3/ZnO/Si was 0.07 nm and 0.2 nm, respectively. The rougher surface in the latter structure leads to a larger surface to volume (*S*/*V*) ratio, which in turn shapes the palladium surface and provides more adsorption sites for hydrogen atoms. As a result, a higher density of dipolar charge can accumulate at the Pd/WO_3 interface, and thus a higher gas sensitivity can be expected [15].

3.2 X-ray photoelectron spectroscopy analysis

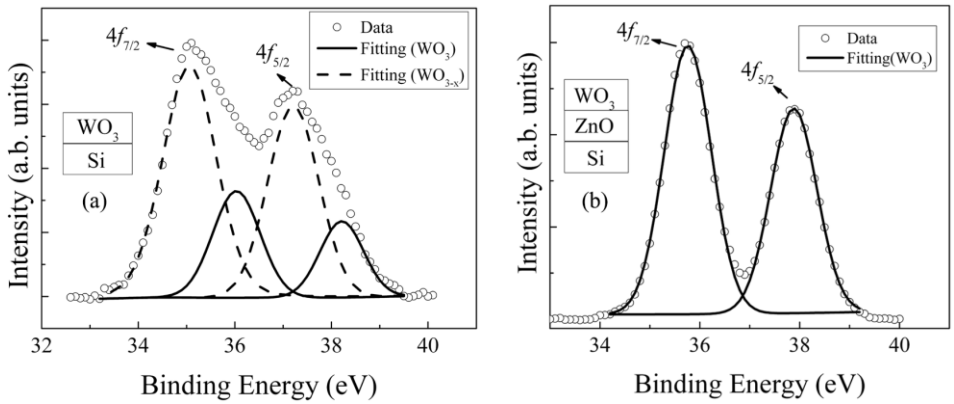

FIG. 3. XPS spectrum and corresponding Gaussian fitting curves of W4*f* in the (a) WO_3/Si and (b) WO_3/ZnO/Si

The stoichiometric composition of the two samples was analyzed by x-ray photoelectron spectroscopy (XPS) and the results are interpreted by the binding energy plots of W4*f* peaks as shown in figure 3. The raw experimental data was first calibrated with carbon (C1*s*) at 285.0 eV to compensate for possible charge effects. Gaussian distributions are employed for the fitting of each peak in the XPS spectrums.

The plot of the WO_3/ZnO/Si (figure 3b) XPS data reveals two peaks: one at 35.9 eV for W4$f_{7/2}$ and the other at 37.9eV for W4$f_{5/2}$ [16]. These peaks suggest that the WO_3 layer on ZnO is highly stoichiometric and fully oxidized which resemble a high population of W^{6+} oxide states. In contrast, the XPS data for WO_3 grown onto Si shows more complex fitting results (figure 3a). The two main peaks (dash line) at binding energy of 35.1 eV and 37.3 eV is attributed to the contribution of W^{5+} states and W^{4+} states which represent a population of sub-stoichiometric WO_{3-x} [17]. The extra fitting peaks at higher binding energy (solid line) can be interpreted as a population of W^{6+} states, in consistency with WO_3/ZnO/Si. Comparing the XPS results, the WO_3 film grown on the silicon surface has a higher density of energy states. This can originate from oxygen vacancies and serve as electron traps that facilitate the trapping of charge from incoming hydrogen adsorbates at the metal/oxide interface [18].

4. Results and discussion

4.1 Static response

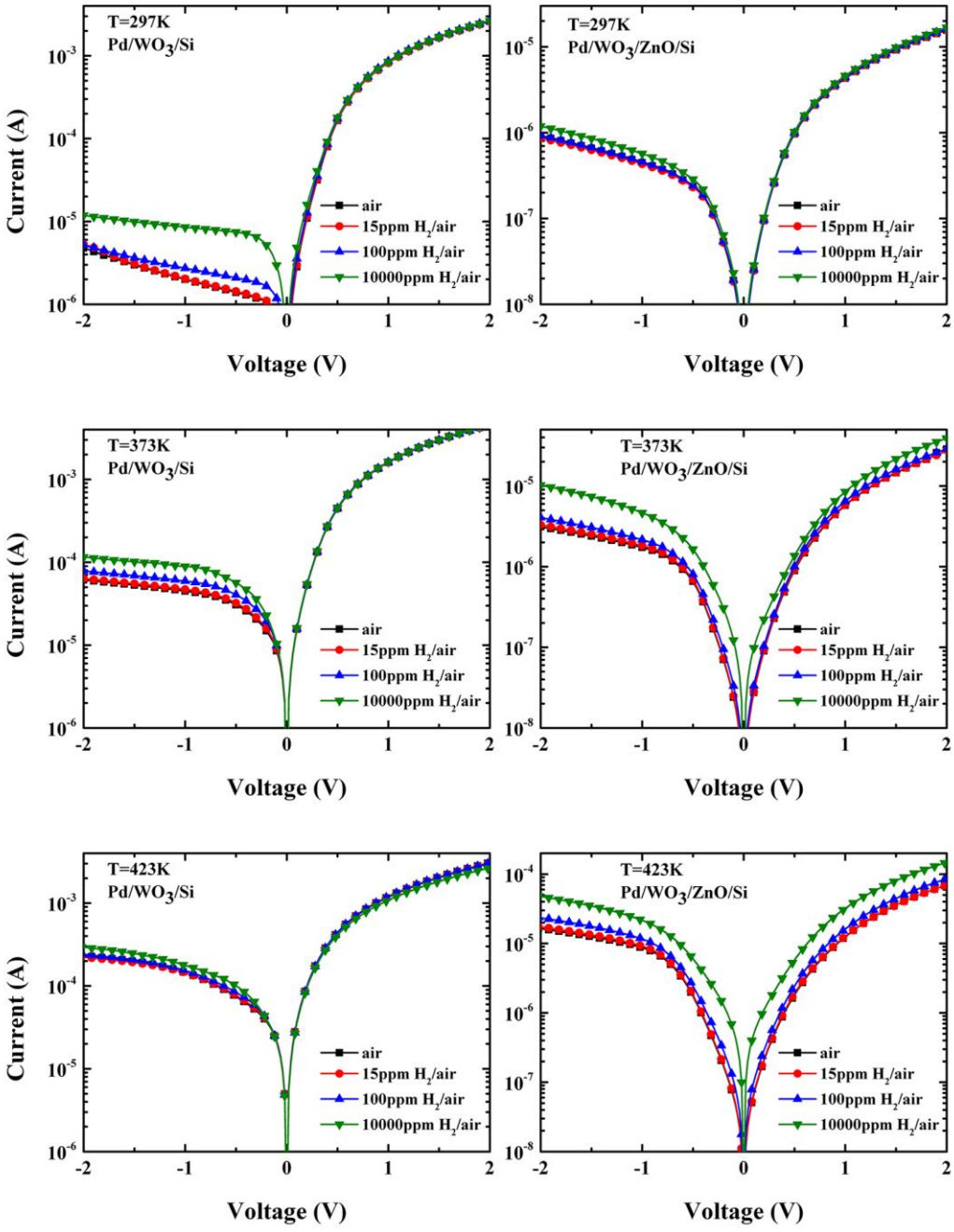

FIG. 4. Current-voltage characteristics of the $Pd/WO_3/Si$ Schottky diode and $Pd/WO_3/ZnO/Si$ Schottky diode when exposed to air and 15 ppm H_2/air, 100 ppm H_2/air and 10000 ppm H_2/air at 300K, 373K and 423K

The current-voltage (*I-V*) characteristics of the $Pd/WO_3/Si$ and $Pd/WO_3/ZnO/Si$ Schottky diodes were measured under exposure to synthetic air and hydrogen gas and shown in figure 4. Different hydrogen concentrations were allowed to flow by balancing 10 000-ppm hydrogen with synthetic air at temperatures of 300 K, 373 K and 423 K,

respectively. For both devices, the forward and reverse currents increase in proportion to hydrogen concentrations, and the lowest hydrogen detection level was chosen as 15 ppm in this investigation. Furthermore, the operating temperature shows a strong influence on the hydrogen detection capability. The Pd/WO_3/Si Schottky diode exhibits hydrogen-sensing properties which functions ideally at reverse bias at low temperature (300 K), meanwhile the Pd/WO_3/ZnO/Si Schottky diode could respond at both forward and reverse biases ideally at high temperature (423 K).

These observations can be explained with the classical thermal emission model. For a Schottky diode with an interfacial oxide layer (MIS type), the *I-V* relation (with $V > 3kT/q$) can be given by [19],

$$I = I_0\left[\exp\frac{q}{nk_BT}(V - IR_s)\right], \quad (1)$$

where V, n, q, k_B, R_S, and T are applied voltage, ideality factor, electron charge, Boltzmann constant, the series resistance and temperature in Kelvin, respectively. I_0 is the reverse saturation current defined as,

$$I_0 = AA^*T^2\exp(-\frac{q\phi_B}{k_BT}), \quad (2)$$

where A is the surface area of Pd metal contact, A^* the effective Richardson constant (120 A/cm^{2}K^2 for *n*-type Si [20]) and ϕ_B the Schottky barrier height. By fitting ln(I) versus V in the low-voltage region , the value of I_0 can be extrapolated from the y-axis intercept for each temperature. The Schottky barrier height, ϕ_B, could be further calculated from Eq. (2). The barrier height in air of the two diodes, $\phi_{B,air}$, and the change in the barrier-height $\Delta\phi_B$, defined as $\phi_{B,H2} - \phi_{B,air}$ with respect to different concentrations of hydrogen gas are shown in the Table I. Due to the presence of hydrogen adsorbates, a decrease in barrier height is expected to the formation of a dipole layer at the Pd/oxide interface [2].

TABLE I. Schottky barrier height $\phi_{B,air}$ and ideality factor n in air and the change of Schottky barrier height $\Delta\phi_B$ in different hydrogen concentrations at 300K, 373K and 423K

	Temperature (K)	ϕ_B (eV)	n	$\Delta\phi_B$ (meV) Concentration (ppm)			
		air	air	15	100	1200	10000
WO_3	300K	0.62	2.45	-0.18	-12.89	-43.78	-46.61
	373K	0.68	2.21	-1.78	-8.64	-17.17	-17.10
	423K	0.75	2.04	-1.57	-3.51	-6.38	-6.37
WO_3/ZnO	300K	0.68	2.55	-0.31	-0.61	-5.13	-4.47
	373K	0.83	2.31	-1.16	-7.56	-33.51	-35.89
	423K	0.92	2.17	-1.34	-14.23	-53.29	-57.59

From the Table I, we can see that the Schottky barrier height in air increased more than 10% within the investigated temperature range after inserting a 40 nm ZnO in the Pd/WO_3/Si diode. The increase of the barrier height with temperature is attributed to the formation of inhomogeneous Schottky barriers [15]. As the concentration of hydrogen increases, more hydrogen molecules will be adsorbed on the Pd surface and a larger barrier height change

was observed. After the hydrogen concentration reaches 1200-ppm H_2/air, however, the hydrogen absorption tends to saturate signifying full adsorbate coverage where the adsorption rate is equal to the rate of depletion at the interface [21].

Another important parameter describing the Schottky didoes is ideality factor, *n*, which can be obtained from the slop of the plot of Ln(*I*) versus *V*, as following equation,

$$n = \frac{q}{k_B T}\frac{d(V)}{dLn(I)}, \tag{3}$$

The ideality factor of the two devices in air is given in Table I. The calculated value is around 2.0 ~ 2.5, approaching the ideal value of 1. However, it is possible that there are some bulk defects in the tungsten oxide and also zinc oxide, including surface defects at the interface between these two materials [22]. As temperature increases, the dominant transport mechanism can be better modeled by the thermionic emission, to the extent that there are a small number of defects present that can contribute to the pinning of the barrier height. This is why there is no considerable change in the *I-V* characteristics and thus the barrier height.

4.2 Discussion of energy band diagram

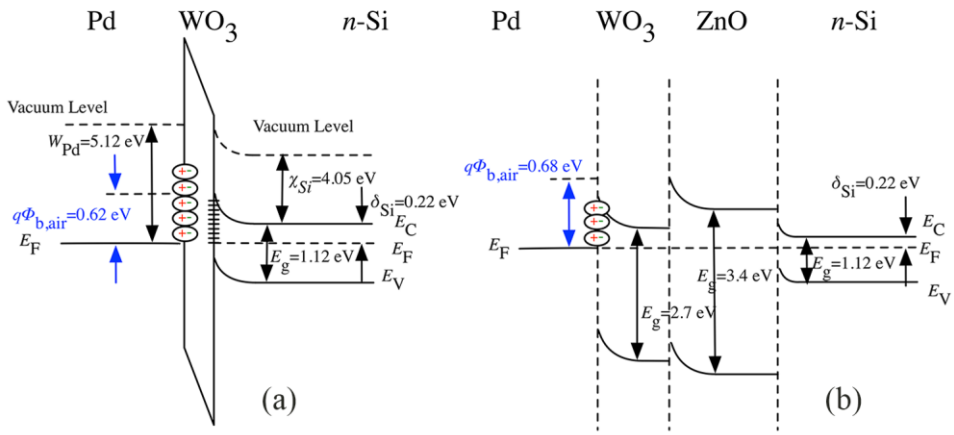

FIG. 5. Energy band diagram of the (a) Pd/WO_3/Si, (b) Pd/WO_3/ZnO/Si Schottky didoes under air ambience

The equilibrium energy-band diagrams of the two Pd/oxide/Si Schottky diodes are shown in figure 5. The bulk Fermi level in the Si substrate referring to the doping density is calculated as, E_F=0.22 eV. As for Pd/WO_3/Si diode, thermally excited electrons can tunnel across the thin WO_3 layer and the barrier height is defined as the potential difference between the Fermi level and the conduction band edge of Si. Here we assume that the Fermi level is pinned at 1/3 above the valance band of the Si [20], about 0.37 eV. Therefore, the corresponding barrier height across the Pd Schottky metal and Si substrate is (1.12 - 0.37) eV = 0.75 eV, roughly consistent with the calculated barrier height at room temperature.

In case of the WO_3-ZnO heterojunction, Anderson model is used to explain the energy-band diagram [23], with the assumption that the interface states can be neglected. The electron affinity of WO_3 and ZnO is 4.92 eV and 4.50 eV, and the band gap of the two oxides is 2.7 eV and 3.4 eV, respectively [24]. With these parameters, we can obtain the theoretical energy band diagram, as shown in figure 5 (b). The electrons need more thermal energy to

jump across - rather than tunnel through - the intermediate oxide layer. Therefore, the barrier height can be defined as the potential difference between the Fermi level and the conduction band edge of ZnO.

When the Schottky diodes are exposed to hydrogen, the hydrogen molecules ($H_{2,\,gas}$) first dissociate into hydrogen atoms (H) via catalytic activity and then absorbed to the adsorption sites on the Pd surface [21]. Some of the dissociated hydrogen atoms react with the oxygen molecules, surface oxygen and hydroxide in the air ambience and form water. The other ones diffuse through the Pd metal layer and Pd/WO_3 interface and then further penetrate into the WO_3 film. The hydrogen atoms interact with the oxygen atom, which are located at Pd/WO_3 interface and inside the WO_3 layer, and form a dipole layer, as shown in figure 5. Such dipole layer raises the Fermi level and lowers the barrier height substantially, allowing more electrons to flow through the oxide layer.

With the above analysis, we next examine the effect of voltage biasing on the hydrogen sensing performance. At forward bias, the barrier seen by electrons in the Si is lower and increasing voltage leads to a rapidly rising forward current. At reverse bias, in contrast, the lifting Fermi level at metal side will increase the built-in voltage in Si and block the flow of electrons from the semiconductor to metal. An increased barrier height at reverse bias permits more dipoles formed at the Pd/oxide interface, thus a bigger barrier height shift was observed at reverse bias for Pd/WO_3/Si sensor. In terms of Pd/WO_3/ZnO/Si, however, the barrier height is pinned by the conduction band edge of ZnO and the rectifying effect was restrained as shown in the *I-V* characteristics, compared with the Pd/WO_3/Si device. As a result, the Pd/WO_3/ZnO/Si shows a significant hydrogen-sensing feature at both forward and reverse bias.

4.3 Dynamic response

The measured dynamic response in terms of current is shown in figure 6. The response of the two sensors upon the exposure and removal of H_2 source with 10 000-ppm concentration in air. These measurements were conducted at different temperatures of 300 K, 373 K and 423 K under a constant reverse bias current of 100 μA. In the response, a voltage shift of 0.26 V, 0.40 V is recorded for the Pd/WO_3/Si diode and for the Pd/WO_3/ZnO/Si diode, 0.5 V and 4.0 V, at 373 K and 423 K respectively.

From the data as shown in figure 6, a response time τ_{res}(90%) and recovery time τ_{rec}(90%) [25] of 125 s and 35 s are recorded for the Pd/WO_3/Si Schottky diode when exposed to 10000-ppm H_2/air at 423 K. Under the same conditions, the Pd/WO_3/ZnO/Si diode exhibits times of 105 s and 25 s, respectively. This signifies that after adding a ZnO layer into the Pd/WO_3/Si device, similar but faster response can be obtained which is expected as the contribution of the rougher surface area of WO_3 sputtered on ZnO layer.

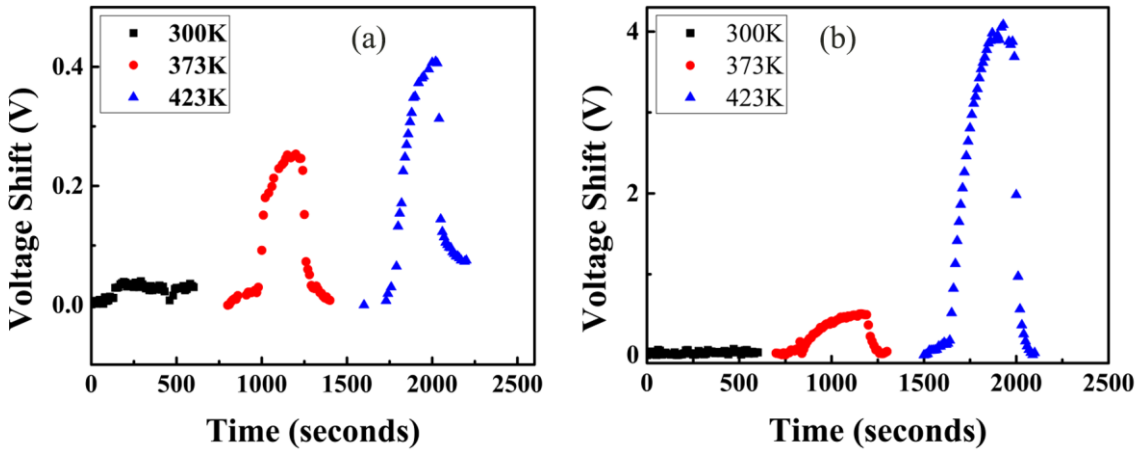

FIG. 6. Voltage shift towards the introduction and removal of 10000 ppm H_2/air gas under constant current of 100 uA (a) Pd/WO_3/Si (b) Pd/WO_3/ZnO/Si

Table II presents a comparison of the studied devices with other MOS-type Schottky diode based hydrogen sensors. The gas sensing performance were all tested towards 1% H_2 in air. Although the response time for the studied sensors is not much shorter than that of other oxide based devices, the WO_3/ZnO heterojunction-type sensor with voltage shift of 4.0 V and recovery time of 25 seconds at bias current of 100 uA, exhibits a superior performance to other devices. In addition, compared with the results of single WO_3 or ZnO based sensor, we may say that the heterojunction structure plays a vital role for the promising hydrogen detecting capabilities.

TABLE II. Summary of the experimental hydrogen sensing results for the MOS-type Schottky diode based sensors

Oxide	*T* (K)	Bias current (uA)	Voltage shift (V)	Response time (s)	Recovery time (s)	Reference
WO_3/ZnO	423	100	4.0	105	25	-
WO_3	423	100	0.40	125	35	-
ZnO	893	1	0.33	108	210	[26]
Ga_2O_3	583	1000	0.21	500	380	[27]
SnO_2	693	1	0.13	105	130	[28]
MoO_3	443	100	1.34	40	270	[29]

5. Conclusion

In conclusion, a WO_3/ZnO heterojunction based Schottky diode hydrogen sensor was fabricated and the energy band diagram distribution was investigated. Compared with the single oxide layer device, AFM and XPS data show that the WO_3 layer grown on the ZnO indicates rougher surface and remains fully stoichiometric after annealing at 823 K. The *I-V* characteristics reveal that the Pd/WO_3/ZnO/Si diode operates favorably at high temperatures (423 K), while the Pd/WO_3/Si device favors operation solely in reverse bias at room temperature. This difference is attributed to the barrier height modulation of WO_3/ZnO

heterojunction. From the transient analysis, the Pd/WO_3/ZnO/Si diode exhibits faster response and recovery towards hydrogen. When reverse biased at constant 100 uA at 423 K, a large voltage shift of 4.0 V is recorded, nearly 10 times larger than that of the Pd/WO_3/Si diode. Overall, the WO_3/ZnO heterojunction structure provides the promise for high-performance Si-based hydrogen sensor applications. Lastly, further work should be carried out to study the influence of the ZnO thickness on the gas sensing performance.

Acknowledgement

This work was supported by the CRCG Small Project Funding (201109176240) and University Development Fund (Nanotechnology Research Institute, 00600009) of the University of Hong Kong.

Reference

[1] Bockris JO. A hydrogen economy. Science 1972;176:1323–3.

[2] Hübert T, Boon-Brett L, Black G, Banach U. Hydrogen sensors – A review. Sensors and Actuators B-Chemical 2011;157:352.

[3] Aroutiounian VM. Hydrogen detectors. Int Sci J Altern Energy Ecol 2005.

[4] Ito K. Hydrogen-Sensitive Schottky-Barrier Diodes. Surface Science 1979;86:345–52.

[5] Spetz AL, Tobias P, Baranzahi A, Martensson P, Lundstrom I. Current status of silicon carbide based high-temperature gas sensors. IEEE Trans Electron Devices 1999;46:561–6.

[6] Kim J, Gila BP, Chung GY, Abernathy CR, Pearton SJ, Ren F. Hydrogen-sensitive GaN Schottky diodes. Solid-State Electronics 2003;47:1069–73.

[7] Tang WM, Leung CH, Lai PT. Improved sensing characteristics of MISiC Schottky-diode hydrogen sensor by using HfO_2 as gate insulator. Microelectronics Reliability 2008;48:1780–5.

[8] Rout CS, Krishna SH, Vivekchand SRC, Govindaraj A, Rao CNR. Hydrogen and ethanol sensors based on ZnO nanorods, nanowires and nanotubes. Chemical Physics Letters 2006;418:586–90.

[9] Coles G, Williams G, Smith B. Selectivity Studies on Tin Oxide-Based Semiconductor Gas Sensors. Sensors and Actuators B-Chemical 1991;3:7–14.

[10] Shafiei M, Yu J, Breedon M, Moafi A, Kalantar-zadeh K, Wlodarski W, et al. Pt/MoO_3 nano-flower/SiC Schottky diode based hydrogen gas sensor. Sensors, 2010 IEEE 2010:354–7.

[11] Ahsan M, Ahmad MZ, Tesfamichael T, Bell J, Wlodarski W, Motta N. Low temperature response of nanostructured tungsten oxide thin films toward hydrogen and ethanol. Sensors and Actuators B-Chemical 2012;173:789–96.

[12] Doucette LD, Santiago F, Moran SL, Lad RJ. Heteroepitaxial growth of tungsten

oxide films on silicon(100) using a BaF_2 buffer layer. Journal of Materials Research 2003;18:2859–68.

[13] Yamazoe N, Shimanoe K. Basic approach to the transducer function of oxide semiconductor gas sensors. Sensors and Actuators B-Chemical 2011;160:1352–62.

[14] Naik AJT, Parkin IP, Binions R. Gas sensing studies of an n-n heterojunction metal oxide semiconductor sensor array based on WO_3 and ZnO composites. Sensors, 2013 IEEE 2013:1–4.

[15] Chen T-Y, Chen H-I, Chiu P-S, Huang C-C, Hsu C-S, Chou P-C, et al. Temperature-dependent properties of Pd/GaN Schottky type hydrogen sensors with Cl_2 plasma surface treatments. Materials Chemistry and Physics 2012;135:150–7.

[16] Ottaviano L, Bussolotti F, Lozzi L, Passacantando M, La Rosa S, Santucci S. Core level and valence band investigation of WO_3 thin films with synchrotron radiation. Thin Solid Films 2003;436:9–16.

[17] Bussolotti F, Lozzi L, Passacantando M, La Rosa S, Santucci S, Ottaviano L. Surface electronic properties of polycrystalline WO_3 thin films: a study by core level and valence band photoemission. Surface Science 2003;538:113–23.

[18] Yu J, Yuan L, Wen H, Shafiei M, Field MR, Liang J, et al. Hydrothermally formed functional niobium oxide doped tungsten nanorods. Nanotechnology 2013;24:495501.

[19] Taşçıoğlu I, Aydemir U, Altındal Ş, Kınacı B, Özçelik S. Analysis of the forward and reverse bias I-V characteristics on Au/PVA:Zn/n-Si Schottky barrier diodes in the wide temperature range. Journal of Applied Physics 2011;109:054502–2.

[20] Sze SM, Ng KK. Physics of Semiconductor Devices. Hoboken, NJ, USA: John Wiley & Sons, Inc; 2006.

[21] Lee C-T, Yan J-T. Sensing mechanisms of Pt/β-Ga_2O_3/GaN hydrogen sensor diodes. Sensors and Actuators B-Chemical 2010;147:723–9.

[22] Mridha S, Basak D. Investigation of a p-CuO/n-ZnO thin film heterojunction for H_2 gas-sensor applications. Semiconductor Science and Technology 2006;21:928–32.

[23] Anderson RL. Germanium-Gallium Arsenide Heterojunctions. IBM Journal of Research and Development 1960;4:283–7.

[24] Carpenter MA, Mathur S, Kolmakov A. Metal Oxide Nanomaterials for Chemical Sensors. New York, NY: Springer New York; 2013.

[25] Chiu S-Y, Huang H-W, Huang T-H, Liang K-C, Liu K-P, Tsai J-H, et al. Comprehensive study of Pd/GaN metal–semiconductor–metal hydrogen sensors with symmetrically bi-directional sensing performance. Sensors and Actuators B-Chemical 2009;138:422–7.

[26] Shafiei M, Yu J, Arsat R, Kalantar-zadeh K, Comini E, Ferroni M, et al. Reversed bias Pt/nanostructured ZnO Schottky diode with enhanced electric field for hydrogen sensing. Sensors and Actuators B-Chemical 2010;146:507–12.

[27] Trinchi A, Wlodarski W, Li YX. Hydrogen sensitive Ga_2O_3 Schottky diode sensor based on SiC. Sensors and Actuators B-Chemical 2004;100:94–8.

[28] Shafiei M, Sadek AZ, Yu J, Arsat R, Kalantar-zadeh K, Yu XF, et al. Hydrogen Gas

Sensing Performance of Pt/SnO_2 Nanowires/SiC MOS Devices. International Journal on Smart Sensing and Intelligent Systems 2008;1.

[29] Shafiei M, Yu J, Breedon M, Motta N, Wu Q, Hu Z, et al. Hydrogen Gas Sensors Based On Thermally Evaporated Nanostructured MoO_3 Schottky Diode: A Comparative Study. 2011 Ieee Sensors 2011:8–11.